Title
Origin of Capacity Degradation of High-Voltage KVPO4F Cathode

Journal
Journal of The Electrochemical Society, 167(11)

ISSN
0013-4651

Authors
Kim, Haegyeom
Tian, Yaosen
Ceder, Gerbrand

Publication Date
2020-01-08

DOI
10.1149/1945-7111/aba54e

Peer reviewed

Journal of the Electrochemical Society

Origin of Capacity Degradation of High-Voltage $KVPO_4F$ Cathode

Journal of The Electrochemical Society, 2020 **167** 110555

Origin of Capacity Degradation of High-Voltage $KVPO_4F$ Cathode

Haegyeom Kim,[1,*,z] Yaosen Tian,[2] and Gerbrand Ceder[1,2,*,z]

[1]*Materials Sciences Division, Lawrence Berkeley National Laboratory, Berkeley, California 94720, United States of America*
[2]*Department of Materials Science and Engineering, University of California, Berkeley, California 94720, United States of America*

Potassium vanadium fluorophosphate ($KVPO_4F$) is one of the most promising cathode candidates for K-ion batteries because of its high specific capacity, voltage, and energy density. However, reducing its capacity fade remains an important challenge. This work leverages structure and electrochemical analysis to understand the capacity degradation mechanism of the $KVPO_4F$ cathode. Interestingly, no structural degradation of the $KVPO_4F$ cathode is detected after 200 cycles in the wide voltage window of 5.0–2.5 V (vs K/K^+). Instead, the capacity degradation is attributed to electrolyte decomposition at high voltage (>4.5 V vs K/K^+), which causes drying of the electrolyte and the formation of insulating layers on the cathode surface, significantly increasing the polarization. The properties of four KPF_6- and carbonate-based K electrolytes are compared, and 0.7 M KPF_6 in ethylene carbonate/propylene carbonate exhibits the highest oxidation stability and results in the best cycling stability for the $KVPO_4$ cathode. These findings suggest that the key to improving the cycling stability of $KVPO_4F$ is to develop novel K electrolytes with even higher oxidation stability.

 [DOI: 10.1149/1945-7111/aba54e]

Manuscript submitted June 8, 2020; revised manuscript received July 3, 2020. Published July 24, 2020.

Grid-level electrochemical energy storage and renewable energy conversion have attracted intense interest as world energy consumption rapidly rises. The U.S. Energy Information Administration (EIA) projects a nearly 50% increase in world energy usage by 2050.[1] Li-ion batteries (LIBs) have long been used to power portable electronics, and their application has now expanded to larger energy storage systems; however, their continued use faces important challenges. It remains debatable whether the available Li resources can meet ever-increasing demands for large-scale energy storage systems. Moreover, the use of expensive Co and Ni in Li cathode materials is a problematic.[2,3] In this regard, K-ion batteries (KIBs) have emerged as an alternative low-cost energy storage system.[4–15] K resources are earth abundant, comprising approximately 2.1% of the Earth's crust (K is the 7th most abundant element in the Earth's crust). Unlike Li cathode materials, K cathode materials do not necessarily contain Co and Ni, as proven by much recent works.[11,13–21] In addition, the standard redox potential of K/K^+ is lower than that of Li/Li^+ by ~0.1 V in carbonate-based electrolytes, indicating that KIBs could have high working voltages, comparable to those of LIBs.[22] Finally, graphite is capable of intercalating K ions reversibly, forming KC_8, and can thus be used as a practically feasible working anode for KIBs.[22–25]

In the early stage of KIB development, layered potassium transition metal oxides (K_xMO_2, M = transition metal) were studied as cathode candidates[12,13,19–21,26–32] because of the success of using layered oxide compounds in LIBs and Na-ion batteries (NIBs).[33–43] Although K layered oxides have shown reversible K de/intercalation behavior, the achievable energy is limited by their sloped voltage curves.[4,12,13,20,27,32,44,45] Such a sloped voltage profile is an intrinsic limitation of K layered oxides, which cannot be overcome by substitution, doping, or nanostructuring. In layered oxides, the alkali-ion and transition-metal layers are stacked alternatively, with alkali ions closely packed in each alkali-ion layer, leading to a short alkali–alkali distance and strong interaction between alkali ions in the same layer. This interaction between alkali ions becomes stronger as the ion size increases.[4,27,46,47] The stronger interaction between K ions than between Na or Li ions leads multiple intermediates as the K content changes during charge/discharge, and a steeply sloped voltage curve.[4,46,47] Thus, polyanion-based compounds have been suggested as alterative K cathode candidates because of their three-dimensional K arrangements and less effective K–K interaction, thereby avoiding the sloped voltage curve.[14,46,48,49] However, it remains challenging to find electrochemically active materials for K cathodes. K ions are not extractable from most K-containing compounds, or only a small amount (<1 K^+ per TM) can be extracted, resulting in a low specific capacity (<100 mAh g^{-1}).[20,27,32,44,50] We suspect that this difficulty in discovering electrochemically active K cathode materials stems from the collapse or significant destabilization of the host structure when the large K ions are extracted.

Among the various K-cathode candidates, $KVPO_4F$ has shown particularly promising properties: a high working voltage (>4.2 V), reversible capacity (>100 mAh g^{-1}), specific energy (~450 Wh kg^{-1}), and fast K mobility in the structure.[46,51–56] A recent cost analysis by Yan and Obrovac,[57] based on the BatPac model from Argonne National Lab,[58] also concluded that $KVPO_4F$ is a better choice than K layered oxides because of its lower estimated cost per energy (150–190 \$ kWh^{-1} for the $KVPO_4F$/graphite system vs 160–215 \$ kWh^{-1} for the K_xMO_2/graphite system), although the cost is still higher than that of the state-of-the-art LIB system. However, reducing the rapid capacity decay of $KVPO_4F$ upon electrochemical cycling remains a challenge.[46] Because the main driver that determines the success of a KIB system is the cycle life, as Yan and Obrovac noted in their annualized capital cost analysis (in terms of \$ kWh^{-1} $year^{-1}$),[57] it is vital to understand the underlying capacity degradation mechanism of the $KVPO_4F$ cathode and to use this knowledge to improve its cycling stability.

Our previous work showed that the cycling stability can be improved by using an oxygen-substituted phase ($K_xVPO_{4+y}F_{1-y}$).[46] However, this strategy sacrifices energy density because of the associated voltage lowering and decreased oxidizable V^{3+} content. Recent work by Liao et al. and Liu et al. showed that the cycling stability of $KVPO_4F$ can be significantly improved by making a carbon coating and carbon composite,[54,59] which is consistent with our previous work that showed that the addition of carbon in a $KVPO_4F$ electrode increases the cycling stability.[46] Chihara et al. demonstrated that the electrolyte selection can also affect the first cycle coulombic efficiency of the $KVPO_4F$ cathode.[52] In their work, using ethylene carbonate/propylene carbonate (EC/PC) as the electrolyte resulted in higher coulombic efficiency than using

*Electrochemical Society Member.
[z]E-mail: haegyumkim@lbl.gov; gceder@berkeley.edu

ethylene carbonate/diethyl carbonate (EC/DEC); however, no noticeable difference in the cycling stability was observed in the voltage range of 5.0–2.0 V for 30 cycles. In addition, Nikitina and colleagues showed that 0.3 M KPF_6 in fluoroethylene carbonate electrolyte has better oxidation stability than the EC/PC system; however, the performance was only evaluated over a very limited number of cycles (5 cycles).[60] Neither of these works was able to demonstrate how the electrolyte selection affects the long-term cycling stability.

In our previous work, we observed that the capacity decay mostly originates from the high-voltage region (>4.5 V), indicating that the capacity degradation should be attributed either to the decomposition of the electrolyte or to an irreversible deformation of the $KVPO_4F$ cathode at high voltage.[46] In our continuing efforts to develop a high-performance KIB system, we in the current study investigate the capacity degradation mechanism of the $KVPO_4F$ cathode. We observe that $KVPO_4F$ is stable upon repeated charge–discharge cycling up to 200 cycles without noticeable crystal structure degradation or crack formation in particles. Instead, we found that most of the capacity degradation originates from the instability of K electrolytes upon oxidation at high voltage (>4.5 V vs K/K^+). We also examined the charge–discharge cycling stability of $KVPO_4F$ in the wide voltage window of 2.5–5.0 V vs K/K^+ using several carbonate-based electrolytes. In general, K salts have low solubility in non-aqueous solvents.[61,62] Therefore, only a few K salts, such as KPF_6 and potassium bis(fluorosulfonyl)amide (KFSA), have been used in the preparation of K electrolytes. KFSA has higher solubility in carbonate solvents than KPF_6 salt and the resultant electrolytes exhibit higher ionic conductivity than KPF_6-based electrolytes.[63] However, the FSA anion has been reported to corrode Al current collectors at high potential >4 V (vs K/K^+),[9,61,63,64] which makes KFSA-based electrolytes impractical for high-voltage K cathodes such as $KVPO_4F$. Although some highly concentrated ether-based K electrolytes have offered significant improvement in the charge–-discharge cycling of $K_2Mn[Fe(CN)_6]$ and $KVOPO_4$ cathodes, their operation voltage is limited to under 4.5 V (vs K/K^+).[63,65] Ionic-liquid K electrolytes have also been studied, and Masese and his colleagues proposed their use for high-voltage K cathodes. However, their charging cut-off voltage did not reach over 4.5 V (vs K/K^+).[66,67] In addition, the use of highly concentrated and ionic-liquid electrolytes will increase the production cost of KIBs. For these reasons, in the current study, we evaluated the effect of electrolyte selection on the cycling stability of a $KVPO_4F$ cathode using four different KPF_6-based electrolytes (KPF_6 in EC/DEC, ethylene carbonate/dimethyl carbonate (EC/DMC), EC/PC, and PC), which are the most commonly used electrolytes for K cathode materials and are considered practical.[61] Among these electrolytes, 0.7 M KPF_6 in EC/PC resulted in the best cycling performance, with the $KVPO_4F$ cathode maintaining ∼75% and ∼63% of the initial discharge capacity after 100 and 200 cycles, respectively.

Experimental

Materials synthesis.—The $KVPO_4F$ powder was prepared using a solid-state method, as described in our previous work.[46] First, VPO_4 was synthesized by reacting $NH_4H_2PO_4$ (11.5 g, 98%, Alfa Aesar), V_2O_5 (9.05 g, >99.6%, Sigma-Aldrich), and carbon black (1.2 g, Super P, Timcal). The precursors were mixed using wet ball-milling in acetone for 12 h and dried overnight at 100 °C. The mixture was then pelletized and sintered at 750 °C for 4 h under continuous Ar flow. Stoichiometric amounts of KF (99.9%, Sigma-Aldrich) and the VPO_4 were homogeneously mixed using a planetary ball mill (Retsch PM200) at 300 rpm for 4 h. The mixture was then pelletized and sintered at 650 °C for 8 h with continuous Ar flow.

Electrochemical measurements.—The electrodes were prepared by mixing the active material (70 wt%), Super P carbon black (Timcal, 20 wt%), and polytetrafluoroethylene binder (PTFE; DuPont, 10 wt%) binder in an Ar-filled glovebox. Test cells were assembled into 2032 coin cells in a glovebox with a two-electrode configuration using a K-metal counter electrode. Grade GF/F film (Whatman, USA) was used as the separator. The GF/F separators were washed with acetone and dried at 70 °C before use. The KPF_6 salt (American Elements, 99.5%) was dried at 150 °C under vacuum for >48 h for preparation of the following K electrolytes: 0.7 M KPF_6 in EC/DEC (anhydrous, 1:1 volume ratio), 0.7 M KPF_6 in EC/PC (anhydrous, 1:1 volume ratio), 0.7 M KPF_6 in EC/DMC (anhydrous, 1:1 volume ratio), and 0.7 M KPF_6 in PC. To remove residual H_2O molecules from the electrolytes, we added molecular sieves to the electrolytes; the molecular sieves were washed with deionized water and dried at 500 °C for over 7 days before use. All the K electrolytes used in this study contained <20 ppm H_2O, as confirmed using the Karl Fischer titration method. The electrochemical tests were performed on a battery testing station (Arbin Instruments) using cathode films with a loading density of ∼4.5 mg cm^{-2}.

Materials characterization.—The crystal structures of the obtained materials were analyzed using X-ray diffraction (XRD, Rigaku Miniflex 600) with Cu Kα radiation. The particle morphology was verified using field-emission scanning electron microscopy (FE-SEM, Zeiss Gemini Ultra-55). Air-free X-ray photoelectron spectroscopy (XPS) measurements were performed on a Thermo Scientific K-Alpha XPS System with a monochromatic Al Kα X-ray source at the Molecular Foundry at Lawrence Berkeley National Laboratory. The sample films were transferred into the XPS system using a Thermo Scientific K-Alpha Vacuum Transfer Module to avoid air exposure. The spectra were acquired with passing energy of 50 eV and a dwell time of 50 ms.

Results

We first examined the electrochemical charge–discharge cycling stability of $KVPO_4F$,, in 0.7 M KPF_6 in EC/DEC, which is the most commonly used K electrolyte.[61] Figs. 1a–1b shows the discharge capacity retention with increasing number of cycles at 20 mA g^{-1} with a voltage cut-off of 5.0–2.5 V. In the first cycle, $KVPO_4F$ delivers a capacity of ∼95 mAh g^{-1}; however, only ∼45 mAh g^{-1} (∼47% retention) is retained after 200 cycles (0.265% fade per cycle). The capacity retention after the initial 30 cycles (∼87% retention) is similar to that reported by Chihara et al. (∼88% retention); however, data for extended cycling was not provided in their study.[52] We also observed a decay of the discharging voltage upon repeated electrochemical cycling, as shown in the inset of Fig. 1a. The average discharge voltage drops from ∼4.1 to ∼3.7 V after 200 cycles. Figure 1c presents the charge–discharge curves using the normalized capacity. The voltage changes oppositely upon charging and discharging; that is, the voltage increases for charging but decreases for discharging upon repeated battery cycling, with the voltage change during discharging being more obvious. We would like to emphasize that such a voltage change, an increase during charging and decrease during discharging, can likely be attributed to an increase of polarization upon cycling. However, we do not fully understand the origin of the asymmetric polarization increase between charging and discharging. If structure degradation of the cathode occurs, voltage lowering during both charging and discharging would be expected, as observed in Li-rich disordered rock-salt cathodes and Ni-rich Li layered cathodes.[68–71] Additionally, we conducted charge–discharge experiments using different voltage cut-offs, 5.0–4.3 V and 4.6–2.5 V, as shown in Fig. 1d. The high voltage cut-off results in significant capacity degradation after 120 cycles (∼38% retention), whereas the low voltage cut-off results in ∼92% retention after 120 cycles. This finding clearly indicates that the capacity degradation mainly originates from the high-voltage region (> 4.3 V vs K/K^+), which is consistent with our earlier observation that cycling between 4.7 and 3.0 V results in better stability than cycling between 5.0 and 3.0 V.[46] The capacity fade of the

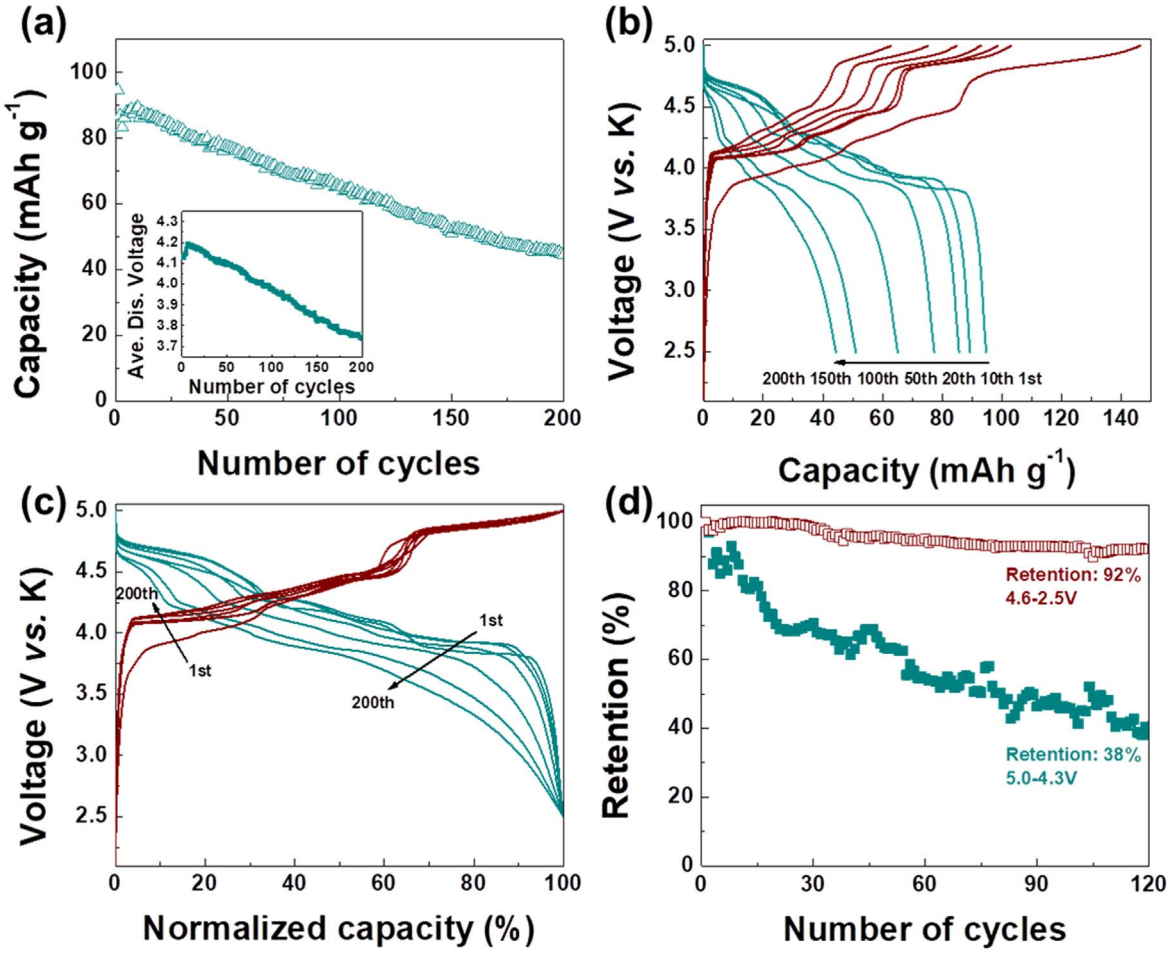

Figure 1. Electrochemical properties of $KVPO_4F$ using 0.7 M KPF_6 in EC/DEC as the electrolyte. (a) Cycling stability of $KVPO_4F$ (inset: average discharge voltage upon charge–discharge cycling). The cut-off voltage is 5.0–2.5 V. (b) Charge–discharge profiles of $KVPO_4F$. (c) Normalized capacity–voltage curves of $KVPO_4F$. (d) Capacity retention of $KVPO_4F$ at different voltage cut-offs.

$KVPO_4F$/K cell could originate from the degradation of the (i) cathode, (ii) anode, or (iii) electrolyte. The role of each component is investigated in the following sections.

The structure stability of the $KVPO_4F$ cathode was studied after repeated charge–discharge cycles. Figure 2a presents ex situ XRD patterns of $KVPO_4F$ before and after 200 cycles when 0.7 M KPF_6 in EC/DEC was used as the electrolyte; no noticeable peak shift or secondary peak evolution are observed (Fig. 2a and inset). The large bump at 10°–30° in the XRD pattern comes from the Kapton tape used to prevent contamination of the samples from air exposure. The oxidation state of vanadium (V) was examined using XPS before and after 200 cycles, as shown in Fig. 2b. No significant peak shift is detected even after 200 cycles. We also examined the morphology change of $KVPO_4F$ using SEM (Figs. 2c–2d). No particle size change or cracks in the particles are observed, consistent with the small volume change of $KVPO_4F$ upon charge and discharge (~6.5%).[46] All of these results indicate that the $KVPO_4F$ cathode does not undergo considerable material degradation even after 200 cycles.

The separator became yellowish and the K metal was covered with black/grey powders after 200 cycles, as shown in Figs. 3a–3b. When we disassembled the cell, the separator was quite dry, which is highly likely due to the decomposition of the electrolyte and the (electro)chemical reaction of the electrolyte with K metal. The black/grey products might originate from either (i) direct reaction of K metal with the electrolyte or (ii) the decomposition products of the electrolyte on the cathode side, which migrate to and deposit on the K metal anode. In the former case, a significant increase of polarization upon cycling in a K/K symmetric cell would be observed, which will be discussed later. Here, we investigated the chemical composition of the decomposed products on the separator qualitatively. The separators before and after cycling were examined using energy-dispersive X-ray spectroscopy (EDS), as shown in Fig. 3c. We immersed the fresh separator in 0.7 M KPF_6 in EC/DEC and dried it inside an Ar-filled glovebox to be used a control. The peak intensity is normalized by Si. Although the peak intensities from Na, Al, and Si do not change as they originate from the glass fiber separator, the C and K signals grow after 200 cycles, likely due to K-electrolyte decomposition and formation of K and C containing products. In addition, no signal from V at ~4.95 keV is observed after 200 cycles (inset of Fig. 3c), indicating that there is no V dissolution from the $KVPO_4F$ cathode. The electrolyte decomposition could lead to deterioration of the cycling performance of $KVPO_4F$/K cells in the following ways: the formation of an insulating layer (i) on the K metal or (ii) on the $KVPO_4F$ cathode could increase the polarization upon cycling, and (iii) electrolyte decomposition itself could also increase the cell resistance and polarization because it will consume the electrolyte in the cell and decrease the ionic conductivity of the electrolyte.

To understand the origin of the capacity degradation in our system using a $KVPO_4F$ cathode and K-metal anode, we evaluated the capacity recovered when the K electrolyte and K-metal anode is refreshed after 200 cycles. For the refreshed cell, we disassembled the cycled cell and assembled a new cell with an unused K-metal anode, K electrolyte, and separator and the cycled $KVPO_4F$ cathode, which is washed with DEC solvent to remove any KPF_6 salt left

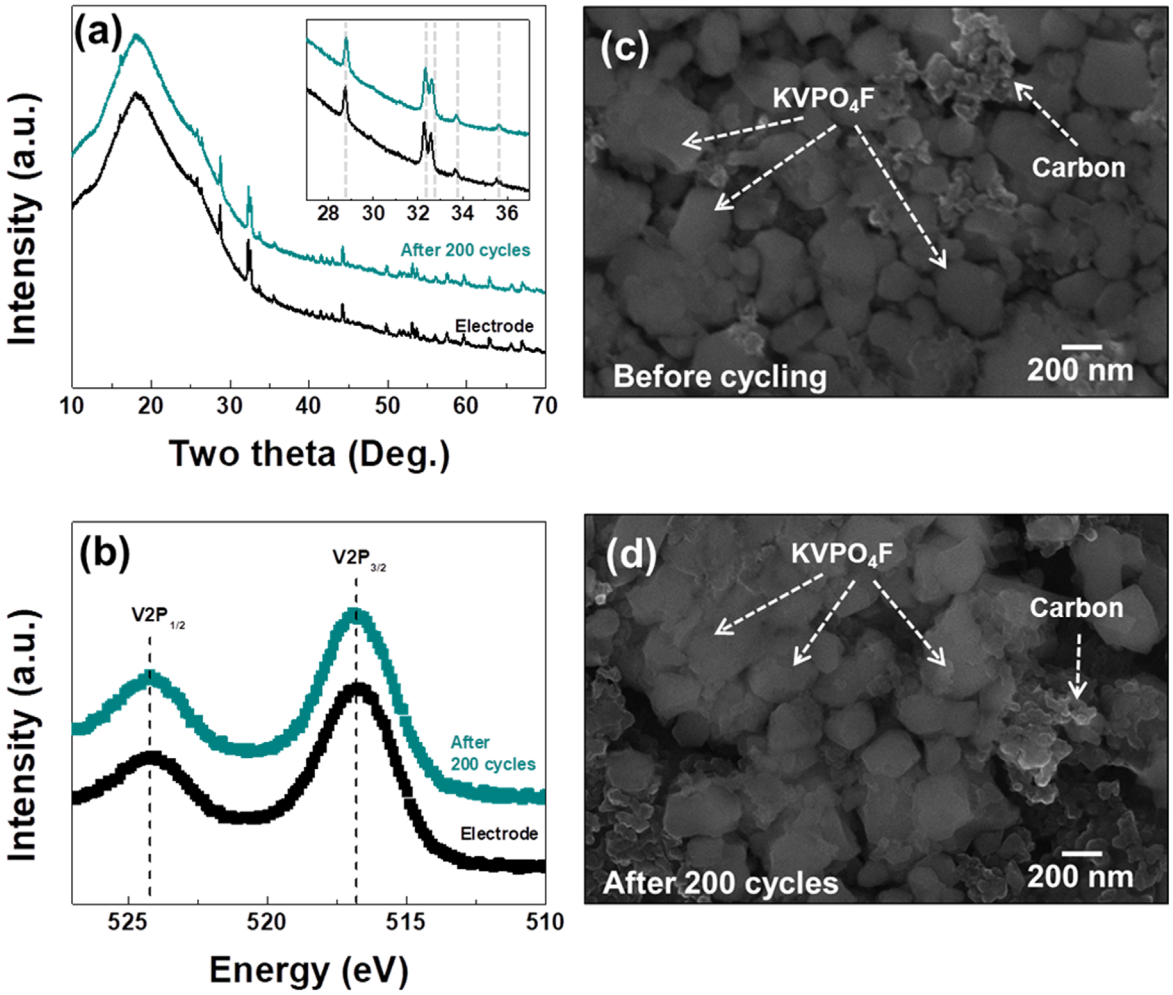

Figure 2. Structure and morphology changes of $KVPO_4F$ cathode upon repeated charge–discharge cycling. (a) XRD patterns and (b) XPS spectra of $KVPO_4F$ cathode before and after 200 cycles. SEM images of $KVPO_4F$ cathode (c) before and (d) after 200 cycles. The smaller particles are carbon additives in the electrode.

behind. The $KVPO_4F$ cathode maintains a capacity of ~45 mAh g^{-1} (~47% retention) after 200 cycles when 0.7 M KPF_6 in EC/DEC electrolyte is used; however, the capacity is recovered to ~69 mAh g^{-1} (~73% retention) after the K electrolyte and K metal are refreshed (Fig. 4a). These results prove that ~50% of the capacity decay comes from the degradation of the K-metal anode and K electrolyte. The remaining 50% might originate from the formation of a resistive layer on the $KVPO_4F$ cathode surface due to the electrolyte decomposition, as we confirmed that there is no structure degradation or dissolution of $KVPO_4F$, as shown in Figs. 2 and 3c. The discharge profile of the refreshed cell is presented in Fig. 4b and remains unchanged compared with that for the 1st cycle of $KVPO_4F$, while there is remaining polarization. This result also demonstrates that the bulk structure of $KVPO_4F$ remains intact after 200 cycles. Figure 4c presents the XPS results of $KVPO_4F$ before and after 200 cycles. The increased peak signals at ~292.2 eV (K–O/K–P binding), ~288.8 eV (C=O binding), and ~286.7 eV (C–O binding) after cycling[72] indicate that the surface layer on the $KVPO_4F$ cathode consists of K–, C–, and O–containing compounds, which might originate from the K–electrolyte decomposition.

The cycling stability of the $KVPO_4F$ cathode was examined in several KPF_6-based carbonate electrolytes (Fig. 4a).[61] The EC/DMC electrolyte shows 59% capacity retention after 140 cycles, and the PC electrolyte results in very rapid capacity degradation with <10% capacity retention after 90 cycles. Thus, both electrolytes are even worse than the EC/DEC system. In contrast, EC/PC offers improved cycling stability, with ~63% of the capacity maintained after 200 cycles (0.185% fade per cycle vs 0.265% fade per cycle with EC/DEC). It is instructive to investigate the correlation between the cycling stability of the $KVPO_4F$/K cells and the oxidation stability of the K electrolytes. Figure 4d presents the linear scan voltammetry (LSV) test results of the KPF_6-based carbonate electrolytes. The LSV tests were conducted at 5 mV s^{-1} from the open-circuit voltage to 5.2 V (vs K/K^+). The oxidation stability trend follows PC > EC/PC > EC/DEC > EC/DMC. The anodic stability of an electrolyte is complex and has been shown to not only depend on the intrinsic oxidation limits of the molecules and ions present, but also on their interaction. The higher oxidation stability of EC/PC over EC/DEC and EC/DMC may be explained by the higher desolvation energy of PC than DEC and DMC.[73] Because PC has larger desolvation energy than DEC and DMC, PC likely participates in solvating K ions along with EC. Given that the solvent molecules that solvate ions have higher oxidation stability than free solvents,[74] it is reasonable that EC/PC has higher oxidation stability than EC/DEC and EC/DMC. Interestingly, the electrolytes with higher oxidation stability offer better cycling stability for the $KVPO_4F$ cathode (Figs. 4a and 4d), except for the PC electrolyte. To determine the stability of K metal using the aforementioned electrolytes and its influence on the cycling stability of $KVPO_4F$/K cells, we tested K/K symmetric cells. Figures 4e–4h presents the charge–discharge profiles of the K/K symmetric cells in various KPF_6-based carbonate electrolytes, in which 5-h charge and 5-h discharge cycles are repeated at ~0.025 mA cm^{-2}. We observed a significantly increased voltage polarization in the PC electrolyte after 200 h (Fig. 4e), indicating that

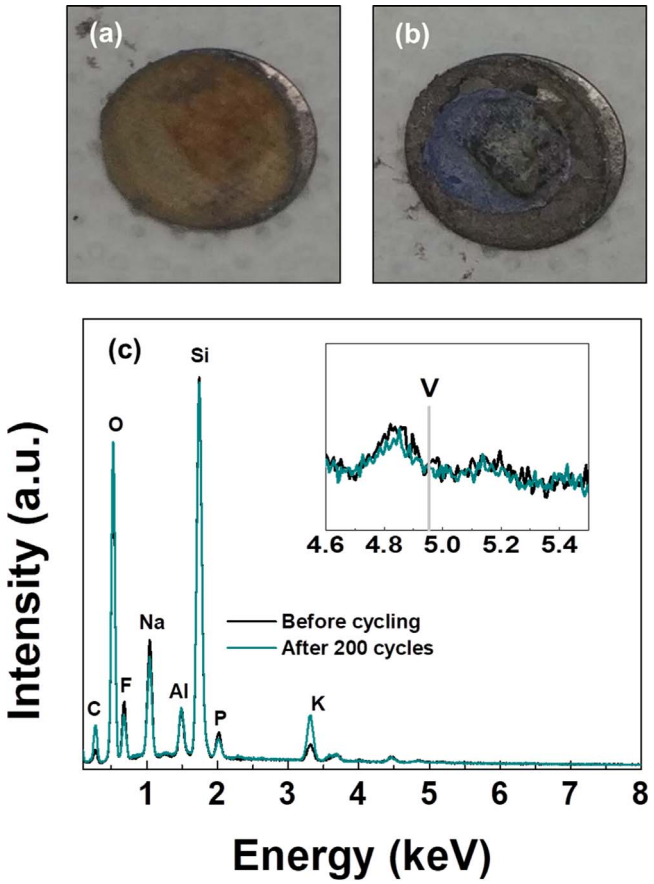

Figure 3. Photographs of (a) separator and (b) K metal after 200 cycles. (c) EDS spectra of separator before and after 200 cycles.

the PC electrolyte is highly reactive with K metal, which may have led to the rapid capacity degradation of the $KVPO_4F$/K cell observed in Fig. 4a. In contrast, the other electrolytes (EC/DEC, EC/PC, EC/DMC) show relatively stable charge–discharge profiles up to 1000 h (100 cycles) while the EC/PC electrolyte system shows the smallest overpotential. The results above indicate that the oxidation stability of K electrolytes is a vital factor in determining the cycling stability of $KVPO_4F$/K cells and that, among the four K electrolytes evaluated, EC/PC is the most promising in terms of improving the cycling stability of the $KVPO_4F$ cathode.

Summary

In this work, the capacity decay mechanism of $KVPO_4F$/K cells was investigated using XRD, XPS, SEM, EDS, and electrochemical characterization. We observe that the bulk structure of the $KVPO_4F$ cathode remains intact even after 200 cycles and argue that electrolyte decomposition and the formation of decomposition products on the cathode surface at high voltage (> 4.5 V) as well as on the anode are responsible for the significant capacity degradation. In addition, we compared the cycling stability of $KVPO_4F$/K cells using four distinct KPF_6- and carbonate-based electrolytes (0.7 M KPF_6 in EC/DEC, EC/DMC, EC/PC, and PC). Among these electrolytes, EC/PC delivers the highest capacity retention (~63%) after 200 cycles (0.185% fade per cycle), which is attributed to its high oxidation stability. This study suggests that $KVPO_4F$ is a highly promising cathode material for large-scale energy storage, but further efforts should be dedicated to the development of novel K electrolytes with high oxidation stability to improve the cycling stability of $KVPO_4F$ cathode for practical use.

Acknowledgments

This work was supported by the BIC (Battery Innovative Contest) program of LG Chem, Ltd. under Contract No.

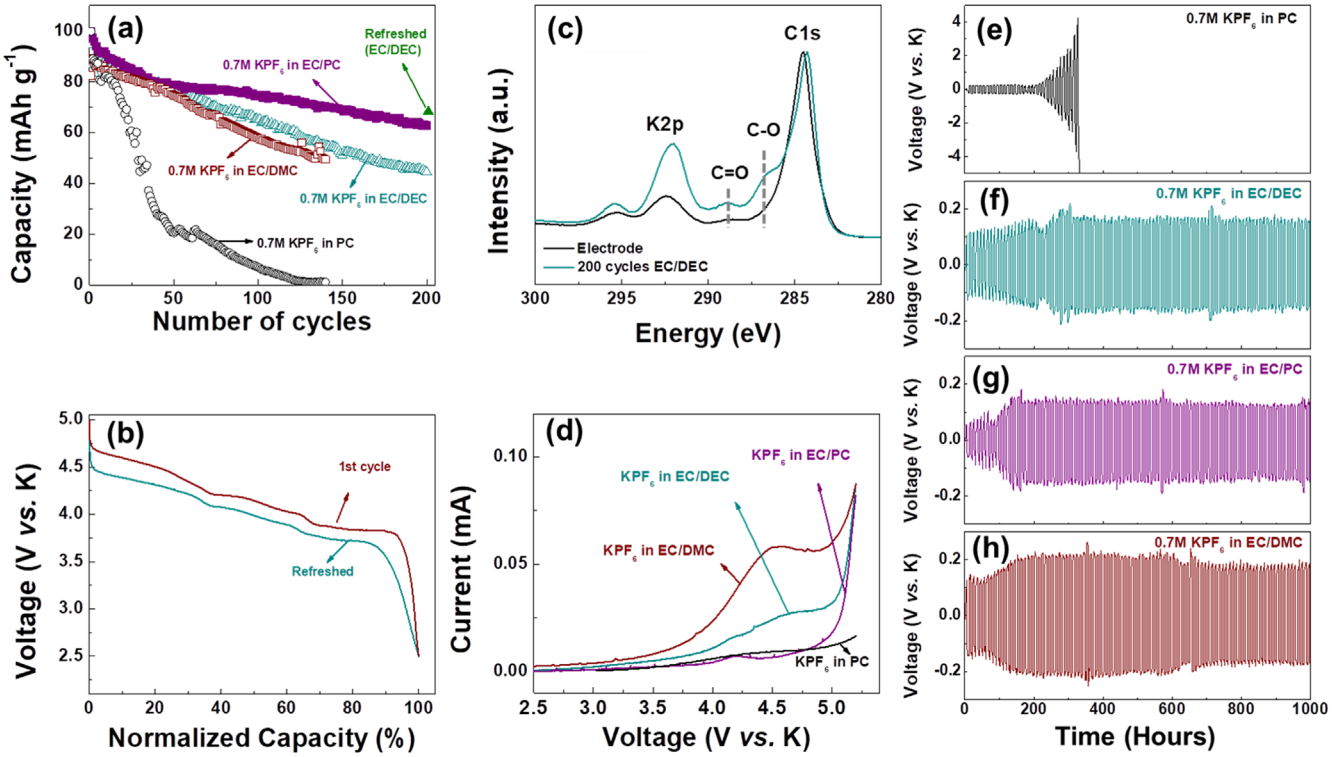

Figure 4. (a). Cycling stability of $KVPO_4F$ cathode in different electrolytes (0.7 M KPF_6 in EC/DEC, 0.7 M KPF_6 in EC/DMC, 0.7 M KPF_6 in EC/PC, and 0.7 M KPF_6 in PC). (b) Discharge profiles of $KVPO_4F$ cathode at the 1st cycle and after refreshing. (c) C_{1s} and K_{2p} regions of XPS spectrum of $KVPO_4F$ cathode before and after 200 cycles. (d) Linear voltage scans of K electrolytes. (e)–(h) Charge–discharge profiles of K/K symmetric cells in different K electrolytes.

20181787. Work at the Molecular Foundry was supported by the Office of Science, Office of Basic Energy Sciences, of the U.S. Department of Energy under Contract No. DE-AC02-05CH11231.

ORCID

Haegyeom Kim https://orcid.org/0000-0002-5962-8244
Gerbrand Ceder https://orcid.org/0000-0001-9275-3605

References

1. U.S. Energy Information Administration, https://eia.gov/todayinenergy/detail.php?id=41433 (2019).
2. E. A. Olivetti, G. Ceder, G. G. Gaustad, and X. Fu, *Joule*, **1**, 229 (2017).
3. X. Fu, D. N. Beatty, G. G. Gaustad, G. Ceder, R. Roth, R. E. Kirchain, M. Bustamante, C. Babbitt, and E. A. Olivetti, *Environ. Sci. & Tech.*, **54**, 2985 (2020).
4. H. Kim, H. Ji, J. Wang, and G. Ceder, *Trends in Chem.*, **1**, 682 (2019).
5. H. Kim, J. C. Kim, M. Bianchini, D.-H. Seo, J. Rodriguez-Garcia, and G. Ceder, *Adv. Energy Mater.*, **8**, 1702384 (2018).
6. J. C. Pramudita, D. Sehrawat, D. Goonetilleke, and N. Sharma, *Adv. Energy Mater.*, **7**, 1602911 (2017).
7. C. Vaalma, D. Buchholz, and S. Passerini, *Current Opinion in Electrochem.*, **9**, 41 (2018).
8. Y.-H. Zhu, X. Yang, T. Sun, S. Wang, Y.-L. Zhao, J.-M. Yan, and X.-B. Zhang, *Electrochem. Energy Rev.*, **1**, 548 (2018).
9. J.-Y. Hwang, S.-T. Myung, and Y.-K. Sun, *Adv. Funct. Mater.*, **28**, 1802938 (2018).
10. R. Rajagopalan, Y. Tang, X. Ji, C. Jia, and H. Wang, *Adv. Funct. Mater.*, **30**, 1909486 (2020).
11. L. Xue, Y. Li, H. Gao, W. Zhou, X. Lü, W. Kaveevivitchai, A. Manthiram, and J. B. Goodenough, *J. Am. Chem. Soc.*, **139**, 2164 (2017).
12. H. Kim, J. C. Kim, S.-H. Bo, T. Shi, D.-H. Kwon, and G. Ceder, *Adv. Energy Mater.*, **7**, 1700098 (2017).
13. H. Kim, D.-H. Seo, J. C. Kim, S.-H. Bo, L. Liu, T. Shi, and G. Ceder, *Adv. Mater.*, **29**, 1702480 (2017).
14. W. B. Park, S. C. Han, C. Park, S. U. Hong, U. Han, S. P. Singh, Y. H. Jung, D. Ahn, K.-S. Sohn, and M. Pyo, *Adv. Energy Mater.*, **8**, 1703099 (2018).
15. X. Jiang, T. Zhang, L. Yang, G. Li, and J. Y. Lee, *Chem. Electro. Chem.*, **4**, 2237 (2017).
16. C. Zhang, Y. Xu, M. Zhou, L. Liang, H. Dong, M. Wu, Y. Yang, and Y. Lei, *Adv. Funct. Mater.*, **27**, 1604307 (2017).
17. Z. Shadike, D.-R. Shi, W. Tian, M.-H. Cao, S.-F. Yang, J. Chen, and Z.-W. Fu, *J. Mater. Chem. A*, **5**, 6393 (2017).
18. T. Deng, X. Fan, J. Chen, L. Chen, C. Luo, X. Zhou, J. Yang, S. Zheng, and C. Wang, *Adv. Funct. Mater.*, **28**, 1800219 (2018).
19. C.-L. Liu, S.-H. Luo, H.-B. Huang, Y.-C. Zhai, and Z.-W. Wang, *Chem. Eng. J.*, **356**, 53 (2019).
20. H. Kim, D.-H. Seo, A. Urban, J. Lee, D.-H. Kwon, S.-H. Bo, T. Shi, J. K. Papp, B. D. McCloskey, and G. Ceder, *Chem.Mater.*, **30**, 6532 (2018).
21. J. Weng, J. Duan, C. Sun, P. Liu, A. Li, P. Zhou, and J. Zhou, *Chem. Eng. J.*, **392**, 123649 (2020).
22. S. Komaba, T. Hasegawa, M. Dahbi, and K. Kubota, *Electrochem. Commun.*, **60**, 172 (2015).
23. J. Liu et al., *Adv. Energy Mater.*, **9**, 1900579 (2019).
24. J. Zhao, X. Zou, Y. Zhu, Y. Xu, and C. Wang, *Adv. Funct. Mater.*, **26**, 8103 (2016).
25. Z. Jian, W. Luo, and X. Ji, *J. Am. Chem. Soc.*, **137**, 11566 (2015).
26. C. Liu, S. Luo, H. Huang, Z. Wang, A. Hao, Y. Zhai, and Z. Wang, *Electrochem. Commun.*, **82**, 150 (2017).
27. Y. Hironaka, K. Kubota, and S. Komaba, *Chem. Commun.*, **53**, 3693 (2017).
28. T. Masese, K. Yoshii, M. Kato, K. Kubota, Z.-D. Huang, H. Senoh, and M. Shikano, *Chem. Commun.*, **55**, 985 (2019).
29. J. U. Choi, J. Kim, J.-Y. Hwang, J. H. Jo, Y.-K. Sun, and S.-T. Myung, *Nano Energy*, **61**, 284 (2019).
30. T. Deng, X. Fan, C. Luo, J. Chen, L. Chen, S. Hou, N. Eidson, X. Zhou, and C. Wang, *Nano Lett.*, **18**, 1522 (2018).
31. X. Wang, X. Xu, C. Niu, J. Meng, M. Huang, X. Liu, Z. Liu, and L. Mai, *Nano Lett.*, **17**, 544 (2017).
32. C. Vaalma, G. A. Giffin, D. Buchholz, and S. Passerini, *J. Electrochem. Soc.*, **163**, A1295 (2016).
33. C. Delmas and L. Croguennec, *MRS Bull.*, **27**, 608 (2011).
34. H. Koga, L. Croguennec, M. Ménétrier, P. Mannessiez, F. Weill, C. Delmas, and S. Belin, *The J. Phys. Chem. C*, **118**, 5700 (2014).
35. N. A. Chernova, M. Ma, J. Xiao, M. S. Whittingham, J. Breger, and C. P. Grey, *Chem. Mater.*, **19**, 4682 (2007).
36. Y.-Y. Wang, Y.-Y. Sun, S. Liu, G.-R. Li, and X.-P. Gao, *ACS Appl. Energy Mater.*, **1**, 3881 (2018).
37. A. Manthiram, J. C. Knight, S.-T. Myung, S.-M. Oh, and Y.-K. Sun, *Adv. Energy Mater.*, **6**, 1501010 (2016).
38. Y. Sun, S. Guo, and H. Zhou, *Adv. Energy Mater.*, **9**, 1800212 (2019).
39. N. Ortiz-Vitoriano, N. E. Drewett, E. Gonzalo, and T. Rojo, *Energy Environ. Sci.*, **10**, 1051 (2017).
40. C. Ma, J. Alvarado, J. Xu, R. J. Clément, M. Kodur, W. Tong, C. P. Grey, and Y. S. Meng, *J. Am. Chem. Soc.*, **139**, 4835 (2017).
41. M. H. Han, E. Gonzalo, G. Singh, and T. Rojo, *Energy Environ. Sci.*, **8**, 81 (2015).
42. S.-W. Kim, D.-H. Seo, X. Ma, G. Ceder, and K. Kang, *Adv. Energy Mater.*, **2**, 710 (2012).
43. H. Kim, H. Kim, Z. Ding, M. H. Lee, K. Lim, G. Yoon, and K. Kang, *Adv. Energy Mater.*, **6**, 1600943 (2016).
44. M. K. Cho, J. H. Jo, J. U. Choi, and S.-T. Myung, *ACS Appl. Mater. Interf.*, **11**, 27770 (2019).
45. H. Kim, D.-H. Kwon, J. C. Kim, B. Ouyang, H. Kim, J. Yang, and G. Ceder, *Chem. Mater.*, **32**, 4312 (2020).
46. H. Kim, D.-H. Seo, M. Bianchini, R. J. Clément, H. Kim, J. C. Kim, Y. Tian, T. Shi, W.-S. Yoon, and G. Ceder, *Adv. Energy Mater.*, **8**, 1801591 (2018).
47. Y. Tian et al., *Chem. Rev.*, , To be submitted (2020).
48. X. Lin, J. Huang, H. Tan, J. Huang, and B. Zhang, *Energy Storage Mater.*, **16**, 97 (2019).
49. H. Park, H. Kim, W. Ko, J. H. Jo, Y. Lee, J. Kang, I. Park, S.-T. Myung, and J. Kim, *Energy Storage Mater.*, **28**, 47 (2020).
50. T. Hosaka, T. Shimamura, K. Kubota, and S. Komaba, *The Chemical Record*, **19**, 735 (2019).
51. S. S. Fedotov, N. R. Khasanova, A. S. Samarin, O. A. Drozhzhin, D. Batuk, O. M. Karakulina, J. Hadermann, A. M. Abakumov, and E. V. Antipov, *Chem. Mater.*, **28**, 411 (2016).
52. K. Chihara, A. Katogi, K. Kubota, and S. Komaba, *Chem. Commun.*, **53**, 5208 (2017).
53. H. Kim, Y. Ishado, Y. Tian, and G. Ceder, *Adv. Funct. Mater>*, **29**, 1902392 (2019).
54. J. Liao, Q. Hu, X. He, J. Mu, J. Wang, and C. Chen, *J. Power Sources*, **451**, 227739 (2020).
55. V. A. Nikitina, S. S. Fedotov, S. Yu. Vassiliev, A. Sh. Samarin, N. R. Khasanova, and E. V. Antipov, *J. Electrochem. Soc.*, **164**, A6373 (2017).
56. D. A. Aksyonov, S. S. Fedotov, K. J. Stevenson, and A. Zhugayevych, *Comput. Mater. Sci.*, **154**, 449 (2018).
57. Z. Yan and M. N. Obrovac, *J. Power Sources*, **464**, 228228 (2020).
58. P. A. Nelson, K. G. Gallagher, I. D. Bloom, and D. W. Dees, *Modeling the Performance and Cost of Lithium-Ion Batteries for Electric-Drive Vehicles* - (Argonne National Lab. (ANL), Argonne, United States of America) Second edition ed.140 (2012).
59. Z. Liu, J. Wang, and B. Lu, *Science Bulletin*, **65**, 1242 (2020).
60. V. A. Nikitina, S. M. Kuzovchikov, S. S. Fedotov, N. R. Khasanova, A. M. Abakumov, and E. V. Antipov, *Electrochim. Acta*, **258**, 814 (2017).
61. T. Hosaka, K. Kubota, A. S. Hameed, and S. Komaba, *Chem. Rev.*, In press (2020).
62. J. Liao, Q. Hu, Y. Yu, H. Wang, Z. Tang, Z. Wen, and C. Chen, *J. Mater. Chem. A*, **5**, 19017 (2017).
63. T. Hosaka, K. Kubota, H. Kojima, and S. Komaba, *Chem. Commun.*, **54**, 8387 (2018).
64. E. Cho, J. Mun, O. B. Chae, O. M. Kwon, H.-T. Kim, J. H. Ryu, Y. G. Kim, and S. M. Oh, *Electrochem. Commun.*, **22**, 1 (2012).
65. N. S. Katorova, S. S. Fedotov, D. P. Rupasov, N. D. Luchinin, B. Delattre, Y.-M. Chiang, A. M. Abakumov, and K. J. Stevenson, *ACS Appl. Energy Mater.*, **2**, 6051 (2019).
66. T. Masese et al., *Nat. Commun.*, **9**, 3823 (2018).
67. K. Yoshii, T. Masese, M. Kato, K. Kubota, H. Senoh, and M. Shikano, *ChemElectroChem*, **6**, 3901 (2019).
68. X. Ju, X. Hou, Z. Liu, H. Zheng, H. Huang, B. Qu, T. Wang, Q. Li, and J. Li, *J. Power Sources*, **437**, 226902 (2019).
69. J. Zheng, P. Xu, M. Gu, J. Xiao, N. D. Browning, P. Yan, C. Wang, and J.-G. Zhang, *Chem. Mater.*, **27**, 1381 (2015).
70. Y. Su, F. Yuan, L. Chen, Y. Lu, J. Dong, Y. Fang, S. Chen, and F. Wu, *J. Energy Chem.*, **51**, 39 (2020).
71. S. H. Song et al., *Adv. Energy Mater.*, **10**, 2000521 (2020).
72. X-ray Photoelectron Spectroscopy (XPS) Reference Pages http://xpsfitting.com/ Accessed May 7th (2020).
73. G. Yoon, H. Kim, I. Park, and K. Kang, *Adv. Energy Mater.*, **7**, 1601519 (2017).
74. J. Wang, Y. Yamada, K. Sodeyama, C. H. Chiang, Y. Tateyama, and A. Yamada, *Nat. Commun.*, **7**, 12032 (2016).